Inorganic Chemistry

pubs.acs.org/IC
Article

En Route to a Molecular Terminal Tin Oxide

Leon Kreßner, Daniel Duvinage, Pim Puylaert, Nico Graw, Regine Herbst-Irmer, Dietmar Stalke, Oliver P. E. Townrow,* and Malte Fischer*

Cite This: *Inorg. Chem.* 2024, 63, 7455−7463
Read Online

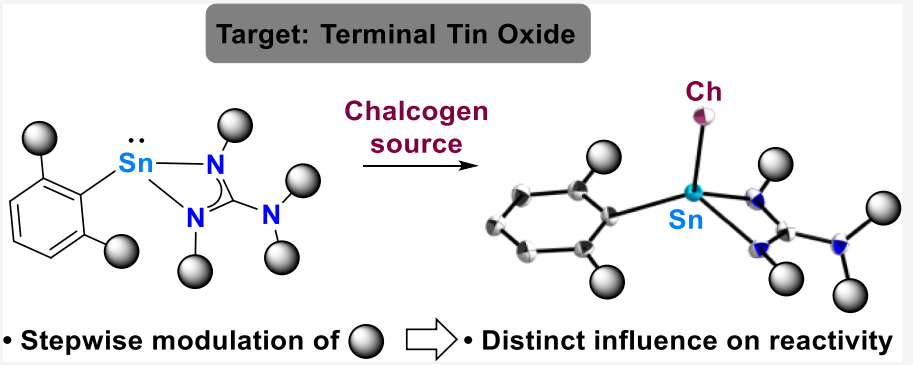

ABSTRACT: In the pursuit of terminal tin chalcogenides, heteroleptic stannylenes bearing terphenyl- and hexamethyldisilazide ligands were reacted with carbodiimides to yield the respective guanidinato complexes. Further supported by quantum chemical calculations, this revealed that the *iso*-propyl-substituted derivative provides the maximum steric protection achievable. Oxidation with elemental selenium produced monomeric terminal tin selenides with four-coordinate tin centers. In reactions with N_2O as oxygen transfer reagent, silyl migration toward putative terminal tin oxide intermediates gave rise to tin complexes with terminal —$OSiMe_3$ functionality. To prevent silyl migration, the silyl groups were substituted with cyclohexyl moieties. This analogue exhibited distinctively different reactivities toward selenium and N_2O, yielding a 1,2,3,4,5-tetraselenastannolane and chalcogenide-bridged dimeric compounds, respectively.

INTRODUCTION

Compounds featuring the carbonyl functionality ($R_2C{=}O$) such as aldehydes, ketones, and amides are fundamental components in organic chemistry. Despite being thermodynamically robust, these functional groups are straightforward to functionalize, given the polarity of the C=O motif. Due to electronegativity differences, their heavier tetrel analogues $R_2E(14){=}O$ (E(14) = silicon, germanium, tin, and lead) exhibit even greater charge separation, which increases down Group 14.[1] Furthermore, significantly weaker π overlap between oxygen and the heavier Group 14 elements results in terminal E(14)=O double bond fragments which are thermodynamically unstable, and often adopt a polarized/ylidic form ($E(14)^+{-}O^-$). The inherent charge disparity in heavier Group 14 carbonyl compounds cannot be quenched effectively by π bond formation, resulting in high reactivity. This is frequently manifested in self-quenching through di-, oligo-, and polymerization reactions; as well as inter and intramolecular C−H activation processes.[2] Consequently, heavier Group 14 carbonyl compounds have been elusive species in the past, leaving ample room for the further development of their chemistry.

Over a century ago, Kipping aimed to synthesize the lightest heavier carbonyls, known as silanones ($R_2Si{=}O$). However, the material produced was later identified to be a polysiloxane, a now omnipresent class of polymers and illustrative of one of the typical self-quenching reactivities, *vide supra*.[3] Despite being detected in low-temperature matrices in the 1980s,[4] it was not until 2007 that the first stable silacarbonyl compounds were reported, utilizing external Lewis acid and/or Lewis base stabilization (Figure 1, I).[5] This strategy paved the way for the isolation of main group carbonyl species across the p-block elements.

Interestingly, the first heavier Group 14 analogue of a ketone, devoid of any acid−base stabilization, was reported for germanium instead of silicon. Tamao, Matsuo, and co-workers achieved this milestone in 2012 with the terminal monomeric germanone,[6a] having paved the way for further examples featuring the terminal Ge=O moiety (Figure 1, II).[6] Within the next seven years, stable compounds featuring the "free" Si=

Received: February 9, 2024
Revised: March 26, 2024
Accepted: March 26, 2024
Published: April 10, 2024

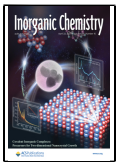

https://doi.org/10.1021/acs.inorgchem.4c00598
Inorg. Chem. 2024, 63, 7455−7463

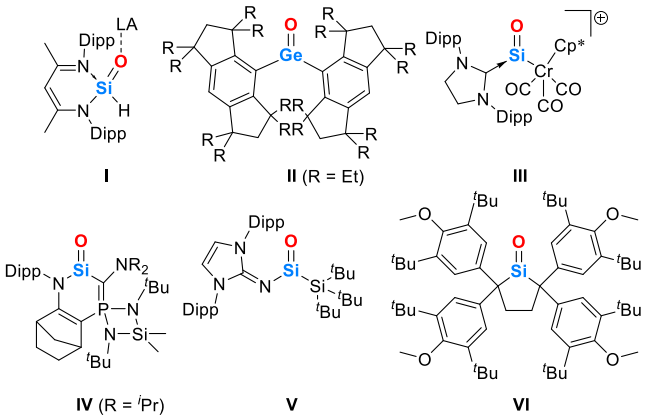

Figure 1. Selected landmark examples of heavier Group 14 carbonyl analogues **I**–**VI** (Dipp = 2,6-^{i}Pr–C_6H_3; LA = Lewis acid).

O functionality were reported by Filippou,[7] Kato,[8] and Inoue[9] (Figure 1, III–V). Iwamoto and co-workers were finally able to tame a cyclic dialkylsilanone, bearing a three-coordinate silicon center with an unperturbed Si=O double bond, utilizing a kinetic stabilization strategy just four years ago (Figure 1, VI).[10]

Such achievements have shifted the perception of these compounds from "laboratory curiosities" to versatile tools for exploring classical carbonyl chemistry with the heavier Group 14 elements and uncovering novel reactivity patterns and applications in oxide ion transfer chemistry.[11]

One intriguing question that remains is whether "true" stannanones/terminal tin oxides are synthetically accessible.[11] The most closely related isolable complexes in literature involve formal "SnO" and "PbO" units trapped by multiple Lewis acid and Lewis base sites.[12]

Herein, we report on our current progress in isolating terminal tin chalcogenides en route to the isolation of a terminal tin oxide.

RESULTS AND DISCUSSION

Heteroleptic stannylenes, comprising one terphenyl and one hexamethyldisilazido ligand of the general type ^{Ar}TerSn{N(SiMe$_3$)$_2$} [**1a**: Aryl(Ar) = Mes (2,4,6-Me$_3$C$_6$H$_2$), **1b**: Ar = Dipp (2,6-^{i}Pr$_2$C$_6$H$_3$)], have recently been found to facilitate the isolation of rare instances of terminal stannaphosphenes and stannaimines.[13] However, when **1a,b** are subjected to typical oxygen transfer reagents, e.g., N_2O or Me_3NO, they yield complex reaction mixtures or undergo decomposition. We postulated that a modified ligand set, featuring a three-coordinate tin atom supported by an intramolecular Lewis base, might provide the necessary electronic and steric characteristics to enable the formation of a heteroleptic stannylene capable of generating terminal tin chalcogenides. In this context, upon inspection of the Frontier Kohn–Sham molecular orbitals of **1**, it becomes evident that **1** can act as an

Scheme 1. (A): Kohn–Sham Molecular Orbitals of 1a,b (BP86/Def2-TZVP); (B) Reactivity of 1a,b towards ^{i}PrN=C=N^{i}Pr to Give the Heteroleptic Terphenyl-/Guanidinato-Stannylenes 2a,b; (C) Molecular Structure of ^{Mes}TerSn{N(^{i}Pr)C(N(SiMe$_3$)$_2$)N(^{i}Pr)} (2a) in the Crystal[a]

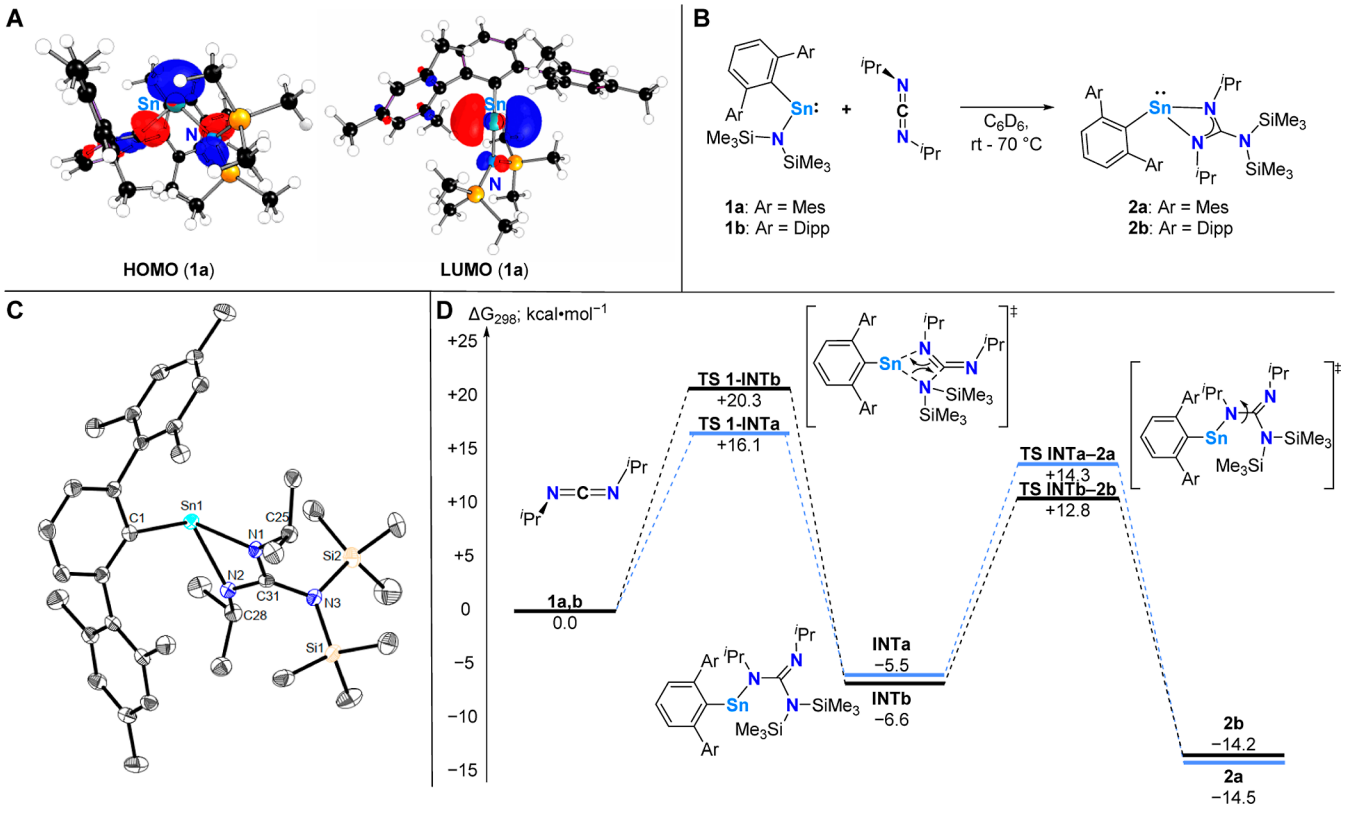

[a]Anisotropic displacement parameters are drawn at the 50% probability level (hydrogen atoms have been omitted for clarity). Selected bond lengths (Å) and angles (deg): Sn1–N1 2.2017(17), Sn1–N2 2.2678(17), Sn1–C1 2.258(2), Sn1···C31 2.638(2), N1–C31 1.331(3), N2–C31 1.329(3), N3–C31 1.421(3), N1–Sn1–C1 104.57(7), N2–Sn1–C1 114.73(7), N1–Sn1–N2 59.19(6), N1–C31–N2 112.20(18); (D) computed mechanism for the formation of **2** from **1** and *N*,*N*-diisopropylcarbodiimide [BP86-D3BJ/Def2-TZVP/Benzene(PCM)].

https://doi.org/10.1021/acs.inorgchem.4c00598
Inorg. Chem. 2024, 63, 7455–7463

Scheme 2. (A) Syntheses of the Terminal Tin Selenides 3a,b; (B) Molecular Structure of ^{Dipp}TerSn(Se){N(^{i}Pr)C(N(SiMe$_3$)$_2$)N(^{i}Pr)} (3b) in the Crystal[a]

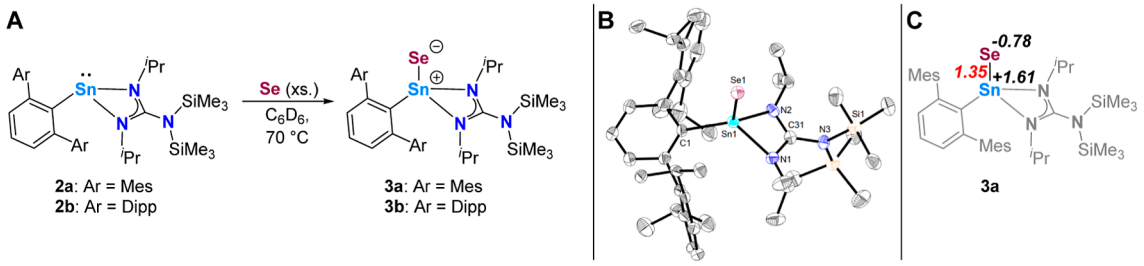

[a]Anisotropic displacement parameters are drawn at the 50% probability level (hydrogen atoms have been omitted for clarity). Selected bond lengths (Å) and angles (deg): Sn1−Se1 2.3818(6), Sn1−N1 2.170(4), Sn1−N2 2.151(4), Sn1−C1 2.184(4), Sn1···C31 2.594(3), N1−C31 1.329(6), N2−C31 1.344(6), N3−C31 1.399(6), N1−Sn1−C1 123.30(16), N2−Sn1−C1 122.82(16), N1−Sn1−N2 61.49(15); (C) tin−Selenium Wiberg bond index (shown in red) and selected natural atomic charges (shown in black) of **3a**.

ambiphile, capable to react nucleophilically either at the tin or nitrogen lone pair observed in the HOMO, and electrophilically at the tin p-orbital observed in the LUMO, which is the major contributor (77%) to the molecular orbital (Scheme 1, A). This consideration, in conjunction with the well-known behavior of carbodiimides, which tend to formally insert into tetrel−amido bonds due to their propensity to act as nucleophiles at nitrogen and electrophiles at carbon,[14] further lays the foundation of our rationale.

Accordingly, the reactivity profiles of **1a,b** toward a range of carbodiimides RN═C═NR (R = Dipp, Me$_3$Si, ^{t}Bu, ^{i}Pr) were investigated. The Dipp-, Me$_3$Si-, and ^{t}Bu-substituted derivatives do not show any reactivity with **1a** even after prolonged periods of heating (c.f. Figures S1−S3),[15] ^{i}PrN═C═N^{i}Pr however readily reacts with both **1a** and **1b** — already starting at room temperature — to solely give the targeted heteroleptic terphenyl-/guanidinato-stannylenes ^{Ar}TerSn{N(^{i}Pr)C(N(SiMe$_3$)$_2$)N(^{i}Pr)} (**2a**: Ar = Mes, **2b**: Ar = Dipp) in isolated yields of up to 89% (Scheme 1, **B**).

Given the selectivity for the formation of **2a,b** on the nature of the carbodiimide substitution pattern, the overall Gibbs free energy of reactions between **1** and carbodiimides of varying R (R = ^{i}Pr, ^{t}Bu, SiMe$_3$) were explored computationally by density functional theory at the BP86-D3BJ/def2-TZVP/Benzene-(PCM) level of theory (Figure S60, Table S12). This found unanimously that only reactions of R = ^{i}Pr were exergonic (ΔG_{298}: ***a***, −14.5 kcal mol^{-1}; ***b***, −14.2 kcal mol^{-1}), presumably due to the increased steric hindrance producing thermodynamically unfavorable products with strained conformations. The endergonic energies for reactions with carbodiimides featuring R = ^{t}Bu, SiMe$_3$ also correlate well to the experimental findings, which showed no conversion to the respective tin guanidinates.[15]

2a and **2b** were characterized by multinuclear nuclear magnetic resonance (NMR) spectroscopy, bulk purity verified by elemental microanalysis, and, in the case of **2a**, single crystal X-ray diffraction (Scheme 1, **C**).

The molecular structure of **2a** shows the three-coordinate tin atom whose coordination environment is distorted trigonal pyramidal [largest bond angle, 114.73(7)° (C1−Sn1−N2)]. The Sn1−N1 and Sn1−N2 bond lengths of 2.2017(17) and 2.2678(17) Å, respectively, differ significantly and are both above respective single bond covalent radii (2.11 Å).[16] Sn1−N2 is elongated compared to other structurally characterized tin guanidinato complexes (c.f. 2.138(3) and 2.185(3) Å in [Sn(Cl){N(*p*-tolyl)C(N(SiMe$_3$)$_2$)N(*p*-tolyl)}]$_2$[17]). The central quaternary carbon atom of the guanidinato ligand is sp^2-hybridized ($\Sigma\angle$ = 359.8°). The characteristic shortening of the carbon−nitrogen bonds of the coordinating κ^2-*N,C,N* moiety of guanidinato ligands compared to the exocyclic carbon−nitrogen bond is clearly pronounced [N1−C31 1.331(3) Å, N2−C31 1.329(3) Å, N3−C31 1.421(3) Å].

The solution NMR data of **2a,b** exhibit two signals for the SiMe$_3$ groups in the respective ^{1}H [δ = 0.03 and 0.18 ppm (**2a**)] and ^{29}Si{^{1}H} [δ = 3.9 and 7.8 ppm (**2a**)] NMR spectra, indicating hindered rotation of the N(SiMe$_3$)$_2$ moiety. Characteristic of guanidinato ligands is the ^{13}C{^{1}H} NMR chemical shift of the central quaternary carbon atom which for **2a,b** are observed at δ^{13}C{^{1}H} = 159.5 (**2a**) and 161.4 (**2b**) ppm, respectively. This is in good accordance with previously reported tin complexes bearing this ligand class.[14,17] The ^{119}Sn{^{1}H} NMR chemical shifts of **2a,b** are located at δ^{119}Sn{^{1}H} = 90.5 (**2a**) and 95.2 (**2b**) ppm, being significantly shifted to lower field when compared to literature guanidinato-tin complexes featuring additional amido ligands (δ^{119}Sn{^{1}H} < −110 ppm[17]), thus demonstrating the influence of the strongly σ-donating terphenyl ligand on the tin atom.

To the best of our knowledge, no studies have been reported to elucidate a mechanism for this transformation. Based on the convenient orbital overlap between the HOMO and LUMO of **1** and the carbodiimide, a metathesis-type process was found to proceed first via a *Sn,N,C,N* heterocyclic transition state ($\Delta G^{\ddagger}_{298}$: Ar = Mes, + 16.1 kcal mol^{-1}; Ar = Dipp, +20.3 kcal mol^{-1}) to produce intermediate **A**, featuring a *Sn,N,C,N* chain (ΔG_{298}: Ar = Mes, −5.5 kcal mol^{-1}; Ar = Dipp, −6.6 kcal mol^{-1}) (Scheme 1, **D**). Intermediate **A** then undergoes a *ca.* 90° torsion around the *Sn,N,C,N* dihedral ($\Delta G^{\ddagger}_{298}$: Ar = Mes, + 14.3 kcal mol^{-1}; Ar = Dipp, + 12.8 kcal mol^{-1}) to form **2** (Overall ΔG_{298}: Ar = Mes, −14.5 kcal mol^{-1}; Ar = Dipp, −14.2 kcal mol^{-1}). Although intermediate **A** is lower in energy than the starting materials, the similarity in energies between **TS1** and **TS2** would preclude its observation even at low temperatures.

In order to assess the suitability of the selected ligand framework for stabilizing terminal chalcogenides in a broader context, **2a,b** were reacted with stoichiometric amounts of elemental selenium (Scheme 2, A). Although no reactions could be observed at room temperature, heating of the reaction mixtures to 70 °C for several hours results in consumption of both starting materials, color changes to a more intense yellow, and main formation of single products according to ^{1}H NMR spectroscopy. It is worth noting that **2a** does not react with

https://doi.org/10.1021/acs.inorgchem.4c00598
Inorg. Chem. 2024, 63, 7455−7463

elemental tellurium in benzene or tetrahydrofuran neither at room temperature nor elevated temperatures of up to 100 °C.

Crystals of **3b** suitable for single crystal X-ray diffraction analysis were obtained from a saturated *n*-hexane solution at −30 °C, confirming the formation of a terminal tin selenide with a four-coordinate tin center, whose coordination environment is best described as distorted tetrahedral (τ_4 = 0.79[18]) (Scheme 2, B). The terminal tin−selenium bond length of 2.3818(6) Å is in good agreement with the double bond covalent radii of the respective elements (Σ_{cov}Sn−Se 2.56 Å, Σ_{cov}Sn = Se 2.37 Å) and is on the shorter end of the tin−selenium bonds reported to date (c.f. Figure S57 and Tbt(Ditp)SnSe 2.373(3) Å;[19d] Tbt = 2,4,6-tris[bis(trimethylsilyl)methyl]phenyl, Ditp = 2,2′-diisopropyl-*m*-terphenyl-2′-yl). Generally, **3a,b** account for the first monomeric and neutral terminal tin selenides with four-coordinate tin centers, with most literature-known derivatives bearing five-coordinate tin centers.[14c,19,20] The aforementioned example with tin in a trigonal planar coordination environment is not obtained directly from the reaction of the respective stannylene precursor with selenium due to the initial formation of a 1,2,3,4,5-tetraselenastannolane and has to be further reacted with three equivalents of triphenylphosphine.[19d] Although the structural parameters of **3b** are indicative of pronounced double bond character of the Sn−Se bond and are usually the preferred way to describe these complexes in the literature,[14c,19] the bonding of **3a** was investigated by computational methods. A Wiberg bond index of 1.35 and natural charges of +1.61 (Sn) and −0.78 (Se) were found, indicating a polarized interaction with a formal order between a single and double bond (Scheme 2, C). Furthermore, natural bond orbital (NBO) analysis was employed and found only two NBOs to describe the Sn−Se interaction with a total of 2.05 electrons, both of which polarized toward Se (60.8%), indicating a zwitterionic single bond. This is consistent with the Sn−N interaction in our previously reported stannaimine systems, taking into account the difference in electronegativity between N and Se.[13b] There are also three NBOs describing lone pairs at Se, accounting for six electrons, one of which is delocalized (86.7% localization on Se). Natural localized molecular orbital analysis shows that a significant amount (12.3%) of the delocalization tail resides in a p-orbital overlap with Sn, explaining the increased Sn−Se bond order above what would be expected for a single bond.

The description of a $Sn^{\delta+}$−$Se^{\delta-}$ single bond with partial charges is in agreement with a weak π-acceptor character of the tin atom and is usually reflected by an upfield shift in the ^{77}Se NMR spectrum (shielded selenium).[19k] The observed ^{77}Se and ^{119}Sn NMR chemical shifts of **3a,b** are observed at δ^{77}Se = −134.6 (**3a**) and −100.6 (**3b**) ppm and δ^{119}Sn = −165.3 (**3a**) and −173.1 (**3b**) ppm,[21] respectively, thus being in the same range as reported for cationic tristannaselone imido clusters, with four-coordinate tin atoms (c.f. δ^{77}Se = −172 ppm and δ^{119}Sn = −133 ppm).[19e]

Having shown that the chosen supporting ligand set at tin is capable of stabilizing terminal tin selenides, terminal tin oxide complexes were targeted next. By pressurizing a C_6D_6 solution of **2a,b** with 1 bar of nitrous oxide at room temperature, and following the reaction by ^{1}H NMR spectroscopy, clean formations of single species over the course of approximately 5 h are observed (Figures S26 and S30).[15] Subsequent workup led to the isolation of colorless solids and liquid injection field desorption ionization mass spectrometry (LIFDI-MS) of the ^{Mes}Ter-substituted derivative is in agreement with the envisioned net oxygen transfer to precursors **2a,b**.[15]

The ^{119}Sn NMR chemical shifts of the obtained compounds are upfield shifted [δ^{119}Sn = −209.9 (**4a**) and −203.7 (**4b**) ppm] when compared to the starting material [δ^{119}Sn = 90.5 (**2a**) and 95.2 (**2b**) ppm] and are in the same range as observed for terminal selenides **3a,b** (*vide supra*). Although the solution NMR and LIFDI-MS data generally support the formation of terminal tin oxides, the ^{29}Si{^{1}H} NMR data indicate different product formation. For the starting material **2a,b**, as well as the terminal tin selenides **3a,b**, the ^{29}Si{^{1}H} NMR spectra each exhibit two signals in close proximity, as expected when both trimethylsilyl groups are located at nitrogen [δ^{29}Si{^{1}H} = 3.9 and 7.8 ppm (**2a**), 4.7 and 7.8 ppm (**2b**), 4.7 and 10.1 ppm (**3a**), 5.5 and 10.9 (**3b**) ppm]. In contrast, the ^{29}Si{^{1}H} NMR of the newly obtained compounds **4a,b** show one signal which is significantly upfield shifted, indicative of different chemical environments of the two silyl moieties [δ^{29}Si{^{1}H} = −23.5 and 10.9 ppm (**4a**), − 23.5 and 10.1 ppm (**4b**)].

This is confirmed by the results of single crystal X-ray diffraction of compound **4b**, clearly demonstrating the formation of compounds with Sn−O−$SiMe_3$ functionalities, and due to silyl migration from the ligand nitrogen to oxygen, the monoanionic guanidinato ligands in **2a,b** are dianionic ligands in **4a,b** (Scheme 3 and Figure 2). Computational

Scheme 3. Reaction of 2a,b with N_2O to Give 4a,b and Overall Reaction Free Energy from 2a,b

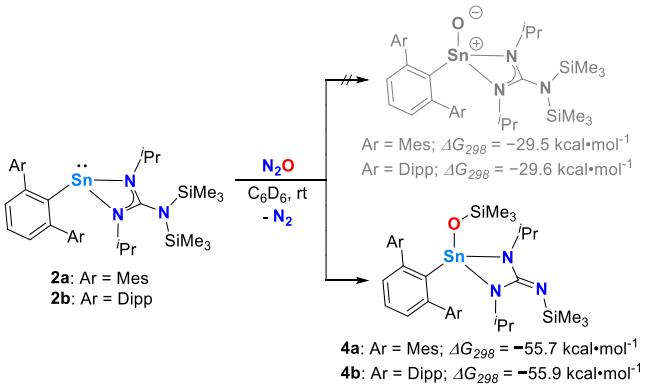

investigation found that the observed products are significantly thermodynamically favored over the targeted terminal oxides by ΔG_{298}: ***a***, −26.2 kcal mol^{-1} and ***b***, −26.3 kcal mol^{-1}.

The tin−nitrogen bond lengths of 2.0466(15) Å (Sn1−N1) and 2.0389(15) Å (Sn1−N2) are approximately 10% shorter than in the starting material, and the exocyclic nitrogen−carbon bond length of 1.263(2) Å (N3−C31) is typical of the formed double bond. The bond length of the newly formed tin−oxygen moiety [1.9427(13) Å] is 10% shorter than the sum of the related single bond covalent radii (Σ_{cov}Sn−O 2.03 Å).

The formal 1,4-silyl migration observed in this study is suggested to occur through a putative terminal tin oxide intermediate, a hypothesis supported by comparable silyl migrations observed in the context of terminal silanones and in our recently reported stannaimine study.[9a,13b,22]

Given this reaction behavior, our focus shifted to a heteroleptic terphenyl-/guanidinato-tin system devoid of silyl groups. Initially, we synthesized the heteroleptic terphenyl-/dicyclohexylamido- stannylene **6** through a salt metathesis reaction between ^{Mes}TerSnCl (**5**)[23] and freshly prepared $LiNCy_2$ (Scheme 4, A).[15] Characterization of **6** was carried

https://doi.org/10.1021/acs.inorgchem.4c00598
Inorg. Chem. 2024, 63, 7455−7463

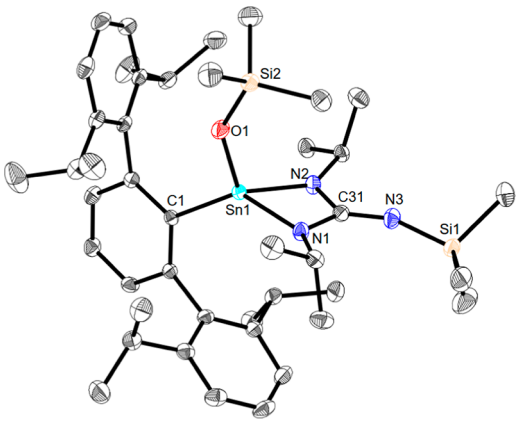

Figure 2. Molecular structure of ^{Dipp}TerSn(OSiMe$_3$){N(^{i}Pr)C(=NSiMe$_3$)N(^{i}Pr)} (**4b**) in the crystal. Anisotropic displacement parameters are drawn at the 50% probability level (hydrogen atoms have been omitted for the sake of clarity). Selected bond lengths (Å) and angles (deg): Sn1−O1 1.9427(13), Sn1−N1 2.0466(15), Sn1−N2 2.0389(15), Sn1−C1 2.1373(17), Sn1···C31 2.5587(18), N1−C31 1.396(2), N2−C31 1.400(2), N3−C31 1.263(2), N3−Si1 1.6762(16), N1−Sn1−C1 134.23(6), N2−Sn1−C1 118.46(6), N1−Sn1−N2 65.94(6), and N1−C31−N2 105.33(14).

out in solution using NMR spectroscopy and in the solid state by single crystal X-ray diffraction.[15]

Additionally, **6** was found to react with *N*,*N*′-diisopropylcarbodiimide, yielding the corresponding guanidinato complex **7**. Notably, this compound can be conveniently synthesized in a one-pot procedure starting from compound **5** (Scheme 4, A). The analytical data for **7** show only marginal differences from those of **2a**,**b**, so that a detailed discussion is omitted at this stage (cf. Scheme 4, B for the structural data).[17]

Interestingly, when **7** was reacted with equimolar amounts of elemental selenium at elevated temperatures (reaction did not initiate at room temperature), most of the compound remained unreacted as confirmed by ^{1}H NMR spectroscopy. Simultaneously, the elemental selenium was entirely consumed, as demonstrated by the absence of any remaining gray precipitate in the reaction mixture. Accordingly, **7** was reacted with an excess of elemental selenium until **7** was completely consumed (Figure S47). From the respective crude ^{1}H NMR spectrum, it was already evident that small amounts of ^{i}PrN═C═N^{i}Pr were liberated. After multiple crystallization attempts, we eventually succeeded in growing both yellow and orange crystals suitable for single crystal X-ray diffraction. The orange crystalline material revealed the formation of 1,2,3,4,5-tetraselenastannolane **8** (Scheme 4, A,C).

Scheme 4. (A) Two-step and One-Pot Synthesis of the Heteroleptic Stannylene 7 and Its Reactivity with Elemental Selenium to Give 8; (B−D) Molecular Structures of ^{Mes}TerSn{N(^{i}Pr)N(Cy$_2$)C(^{i}Pr)} (7), ^{Mes}TerSn(Se$_4$){N(^{i}Pr)C(NCy$_2$)N^{i}Pr} (8), and ^{Mes}TerSn(NCy$_2$)(μ-Se$_2$)Sn{N(^{i}Pr)C(NCy$_2$)N(^{i}Pr)}^{Mes}Ter (9) in the Crystal[a]

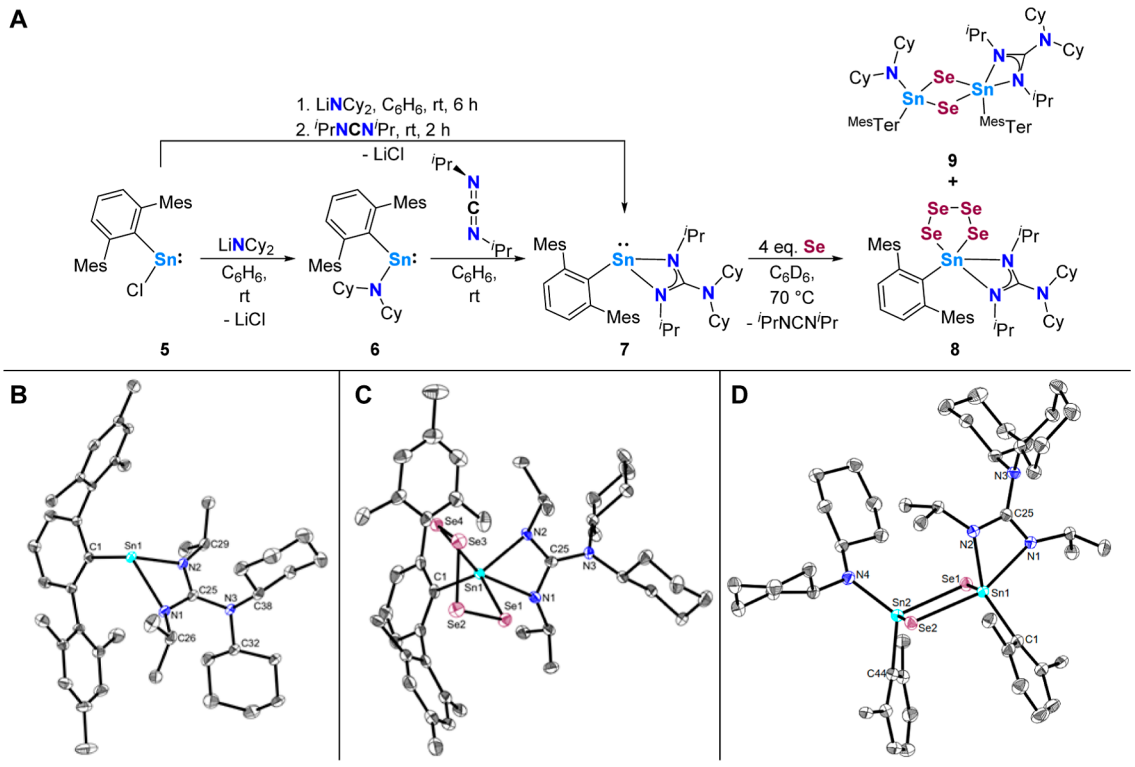

[a]Anisotropic displacement parameters are drawn at the 50% probability level (hydrogen atoms, mesityl functionalities, second molecule (compound **7**) and lattice solvent (compound **7** and **9**) have been omitted for clarity) selected bond lengths (Å) and angles (deg): (B) Sn1−N1 2.2654(12), Sn1−N2 2.1871(13), Sn1···C25 2.6478(15), N1−C25 1.3377(19), N2−C25 1.3250(18), N3−C25 1.4179(18), N1−Sn1−C1 111.83(5), N2−Sn1−C1 99.20(5), N1−Sn1−N2 59.56(5), N1−C25−N2 112.39(12); (C) Sn1−Se1 2.5654(7), Sn1−Se4 2.6520(6), Sn1−N1 2.315(3), Sn1−N2 2.152(4), Sn1−C1 2.183(4), Se1−Se2 2.3276(7), Se2−Se3 2.3244(7), Se3−Se4 2.3400(8), N1−C25 1.324(5), N2−C25 1.354(5), N3−C25 1.391(5), Se1−Sn1−Se4 99.89(2), N1−Sn1−C1 98.69(14), N2−Sn1−C1 120.96(16), N1−Sn1−N2 59.64(13), N1−C25−N2 112.4(4); (D) Sn1−Se1 2.5582(5), Sn1−Se2 2.6315(4), Sn1−N1 2.2877(16), Sn1−N2 2.1543(16), Sn1−C1 2.2132(19), Sn2−Se1 2.5542(4), Sn2−Se2 2.5224(5), Sn2−N4 2.0452(17), Sn2−C44 2.1975(19), C25−N1 1.314(2), C25−N2 1.347(2), C25−N3 1.418(2).

https://doi.org/10.1021/acs.inorgchem.4c00598
Inorg. Chem. 2024, 63, 7455−7463

Scheme 5. (A) Reaction of 7 with N_2O to Give 10; (B) Molecular Structure of ^{Mes}TerSn{N(^{i}Pr)C(NCy$_2$)N^{i}Pr}(μ-O$_2$)Sn{N(^{i}Pr)C(NCy$_2$)N^{i}Pr}^{Mes}Ter (10) in the Crystal[a]

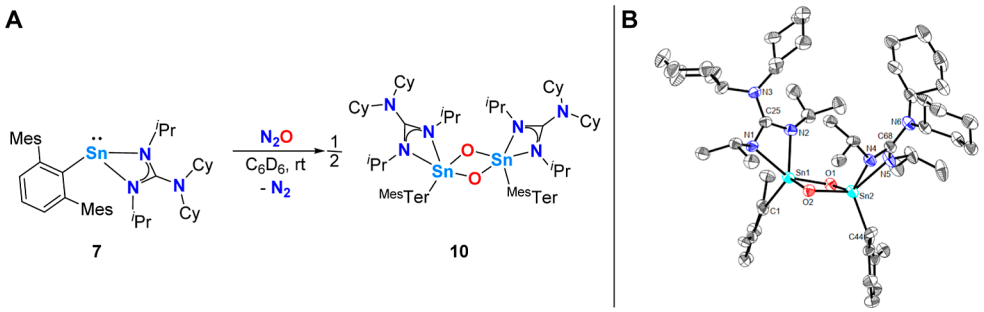

[a]Anisotropic displacement parameters are drawn at the 50% probability level (hydrogen atoms, mesityl functionalities, and lattice solvent have been omitted for clarity). Selected bond lengths (Å) and angles (deg): Sn1−O1 2.039(3), Sn1−O2 1.984(3), Sn1−N1 2.269(3), Sn1−N2 2.140(3), Sn1−C1 2.185(4), Sn2−O1 1.988(3), Sn2−O2 2.052(3), Sn2−N4 2.160(3), Sn2−N5 2.236(4), Sn2−C44 2.193(5), N1−C25 1.338(5), N2−C25 1.350(5), N3−C25 1.393(5), N4−C68 1.358(5), N5−C68 1.329(5), N6−C68 1.395(5), O1−Sn1−O2 82.10(11), O1−Sn2−O2 81.67(11), Sn1−O1−Sn2 97.73(11), Sn1−O2−Sn2 97.39(11).

The structural data within the $SnSe_4$ linkage is in good agreement with the also structurally characterized 1,2,3,4,5-tetraselenastannolane Tbf(Mes)SnSe$_4$ (Sn−Se$_{av}$ 2.58 Å, Se−Se$_{av}$ 2.31 Å).[19d,24] The coordination environment at tin is best described as square pyramidal, according to the structural parameter τ_5 (0.04).[25] The identity of the yellow crystalline material explains why free ^{i}PrN═C═N^{i}Pr was detected in the crude NMR spectra of the reaction and is linked to the formation of the selenium-bridged dimer (1,3,2,4-diselenadistannetane) ^{Mes}TerSn(NCy$_2$)(μ-Se$_2$)Sn{N(^{i}Pr)C(NCy$_2$)N(^{i}Pr)}^{Mes}Ter (**9**) with the terphenyl substituents in a *cis* configuration (Scheme 4, A,D). To the best of our knowledge, the release of carbodiimides from guanidinato ligands upon addition of another substrate has not been observed so far. Although **8** and **9** invariably cocrystallized in our hands, small amounts of **8** could be separated and further analyzed by elemental microanalysis, ^{1}H and ^{119}Sn{^{1}H} NMR spectroscopy (δ119Sn{^{1}H} = −252.9 ppm) (Figures S46, S48 and S49).[15]

The reactivity of **2a,b** and **7** toward elemental selenium differs significantly despite comparatively small differences in backbone substitution patterns.

In this context, we finally investigated the reactivity of **7** toward N_2O.

The reaction is overall clean and results in the formation of a single product according to ^{1}H NMR spectroscopy (Figure S52). Removal of all volatile components and recrystallization from *n*-hexane yields a colorless microcrystalline solid which was first analyzed by LIFDI mass spectrometry and is in agreement with the formation of the oxygen bridged dimer ^{Mes}TerSn{N-(^{i}Pr)N(Cy$_2$)C(^{i}Pr)}(μ-O$_2$)Sn{N(^{i}Pr)-N(Cy$_2$)C(^{i}Pr)}^{Mes}Ter (1,3,2,4-dioxadistannetane) (**10**) (Scheme 5, A).[15] The *cis* configuration of both, the terphenyl and guanidinato ligands, could further be verified by single crystal X-ray diffraction with crystals obtained from a saturated *n*-pentane solution of **10** stored at −30 °C (Scheme 5, B).

Computational investigation found that the dimerization of the proposed terminal oxide intermediate to dimer 10 is exergonic by ΔG_{298} = −26.2 kcal mol^{-1}. The observed *cis* configuration is, albeit only slightly, thermodynamically favored over its trans configuration by ΔG_{298} = −1.4 kcal mol^{-1}.

CONCLUSIONS

We present the reactions of heteroleptic terphenyl-/amido-substituted stannylenes **1a,b** with carbodiimides. Investigated through combined experimental and computational studies, **1a,b** react with the *iso*-propyl-substituted derivative, yielding the corresponding guanidinato complexes **2a,b**. Sterically more demanding carbodiimides are unable to undergo a comparable metathesis-type reaction. Consequently, **2a,b** offers maximum steric protection, which should ultimately facilitate the targeted synthesis of terminal tin chalcogenides.

Compounds **2a,b** react cleanly with elemental selenium to give respective terminal tin selenides **3a,b**. By contrast, in reactions with N_2O as an oxygen transfer reagent, instead of yielding a terminal tin oxide, silyl migration of the guanidinato ligand to the putative tin−oxygen moiety occurs, yielding the corresponding tin complexes **4a,b**, bearing the Sn−OSiMe$_3$ functionality.

To prevent silyl migration, tin compound **7** with an aliphatic cyclohexyl substitution pattern instead of SiMe$_3$ groups was successfully synthesized. Reacting **7** with elemental selenium does not lead to the formation of a terminal tin selenide and gives rise to both the 1,2,3,4,5-tetraselenostannolane **8** and 1,3,2,4-diselenadistannetane **9**, the formation of which is accompanied by the release of ^{i}PrN═C═N^{i}Pr.

The reaction of **7** with N_2O also deviates significantly from those of **2a,b**, leading to the clean formation of the 1,3,2,4-dioxadistannetane **10**, showing that comparatively small changes in substitution have a significant influence on the reaction outcome and further emphasize the difficulties in stabilizing a compound with a terminal tin−oxygen bond.

The obtained compounds have been comprehensively characterized in solution and in the solid state, including single crystal X-ray diffraction of one compound of each accessed class. The bonding situation in the first examples of four-coordinate terminal tin selenide **4a,b** was further analyzed by quantum chemical calculations.

ASSOCIATED CONTENT

Supporting Information

The Supporting Information is available free of charge at https://pubs.acs.org/doi/10.1021/acs.inorgchem.4c00598.

Experimental, crystallographic, and computational details (PDF)

https://doi.org/10.1021/acs.inorgchem.4c00598
Inorg. Chem. 2024, 63, 7455−7463

Accession Codes

CCDC 2330043−2330050 contains the supplementary crystallographic data for this paper. These data can be obtained free of charge via www.ccdc.cam.ac.uk/data_request/cif, or by emailing data_request@ccdc.cam.ac.uk, or by contacting the Cambridge Crystallographic Data Centre, 12 Union Road, Cambridge CB2 1EZ, UK; fax: + 44 1223 336033.

AUTHOR INFORMATION

Corresponding Authors

Oliver P. E. Townrow − *Inorganic and Organometallic Chemistry, Friedrich-Alexander-Universität Erlangen-Nürnberg, D-91058 Erlangen, Germany;* orcid.org/0000-0001-9556-6450; Email: oliver.townrow@fau.de

Malte Fischer − *Institut für Anorganische Chemie, Georg-August-Universität Göttingen, D-37077 Göttingen, Germany;* orcid.org/0000-0002-2806-1302; Email: malte.fischer@uni-goettingen.de

Authors

Leon Kreßner − *Institut für Anorganische Chemie, Georg-August-Universität Göttingen, D-37077 Göttingen, Germany;* orcid.org/0000-0001-9646-5125

Daniel Duvinage − *Institut für Anorganische Chemie und Kristallographie, Universität Bremen, D-28359 Bremen, Germany;* orcid.org/0000-0002-9387-7172

Pim Puylaert − *Institut für Anorganische Chemie und Kristallographie, Universität Bremen, D-28359 Bremen, Germany;* orcid.org/0000-0003-3397-2677

Nico Graw − *Institut für Anorganische Chemie, Georg-August-Universität Göttingen, D-37077 Göttingen, Germany;* orcid.org/0000-0001-8772-8325

Regine Herbst-Irmer − *Institut für Anorganische Chemie, Georg-August-Universität Göttingen, D-37077 Göttingen, Germany*

Dietmar Stalke − *Institut für Anorganische Chemie, Georg-August-Universität Göttingen, D-37077 Göttingen, Germany;* orcid.org/0000-0003-4392-5751

Complete contact information is available at: https://pubs.acs.org/10.1021/acs.inorgchem.4c00598

Notes

The authors declare no competing financial interest.

Additional references are cited in the Supporting Information.[26−41]

Note on safety precautions: compounds containing tin and selenium may pose risks to health and the environment if mishandled or improperly disposed of, and exposure to these compounds could result in adverse health effects. Therefore, manipulations and reactions should be conducted under inert conditions in monitored fume hoods or in an inert-atmosphere dry box while wearing appropriate protective clothing.

ACKNOWLEDGMENTS

Financial support (VCI Liebig fellowship for M.F., Alexander von Humboldt postdoctoral fellowship for O.P.E.T., the University of Bremen central research development fund for P.P.) is gratefully acknowledged. M. F. expresses immense gratitude to Rüdiger Beckhaus, Christian Hering-Junghans, Jens Beckmann, and Simon Aldridge for their invaluable and continuous support, which is crucially connected to the start of his independent career.

REFERENCES

(1) Pauling, L. The Nature of the Chemical Bond. IV. The Energy of Single Bonds and the Relative Electronegativity of Atoms. *J. Am. Chem. Soc.* **1932**, *54*, 3570−3582.

(2) See for example: (a) Kudo, T.; Nagase, S. Theoretical study of silanone. Thermodynamic and kinetic stability. *J. Phys. Chem.* **1984**, *88*, 2833−2840. (b) Kudo, T.; Nagase, S. Theoretical study on the dimerization of silanone and the properties of the polymeric products (H2SiO)n (n = 2,3, and 4). Comparison with dimers (H2SiS)2 and (H2CO)2. *J. Am. Chem. Soc.* **1985**, *107*, 2589−2595.

(3) (a) Kipping, F. S.; Lloyd, L. L. XLVII.-Organic derivatives of silicon. Triphenylsilicol and alkyloxysilicon chlorides. *J. Chem. Soc. Trans.* **1901**, *79*, 449−459. (b) Robison, R.; Kipping, F. S. XLIII.—Organic derivatives of silicon. Part V. Benzylethylsilicone, dibenzylsilicone, and other benzyl and benzylethyl derivatives of silicane. *J. Chem. Soc. Trans.* **1908**, *93*, 439−456.

(4) (a) Arrington, C. A.; West, R.; Michl, J. On the proposed thermal interconversion of matrix-isolated dimethylsilylene and 1-methylsilene: their reactions with oxygen atom donors. *J. Am. Chem. Soc.* **1983**, *105*, 6176−6177. (b) Withnall, R.; Andrews, L. Infrared spectroscopic evidence for silicon-oxygen double bonds: silanone and the silanoic and silicic acid molecules. *J. Am. Chem. Soc.* **1985**, *107*, 2567−2568. (c) Glinski, R. J.; Gole, J. L.; Dixon, D. A. Oxidation processes in the gas-phase silane-ozone system. Chemiluminescent emission and the molecular structure of H2SiO. *J. Am. Chem. Soc.* **1985**, *107*, 5891−5894.

(5) Selected examples: (a) Yao, S.; Xiong, Y.; Brym, M.; Driess, M. An Isolable Silanoic Ester by Oxygenation of a Stable Silylene. *J. Am. Chem. Soc.* **2007**, *129*, 7268−7269. (b) Yao, S.; Brym, M.; van Wüllen, C.; Driess, M. From a Stable Silylene to a Mixed-Valent Disiloxane and an Isolable Silaformamide-Borane Complex with Considerable Silicon-Oxygen Double-Bond Character. *Angew. Chem., Int. Ed.* **2007**, *46*, 4159−4162. (c) Xiong, Y.; Yao, S.; Driess, M. An Isolable NHC-Supported Silanone. *J. Am. Chem. Soc.* **2009**, *131*, 7562−7563. (d) Xiong, Y.; Yao, S.; Driess, M. Silicon Analogues of Carboxylic Acids: Synthesis of Isolable Silanoic Acids by Donor-Acceptor Stabilization. *Angew. Chem., Int. Ed.* **2010**, *49*, 6642−6645. (e) Xiong, Y.; Yao, S.; Müller, R.; Kaupp, M.; Driess, M. Activation of Ammonia by a Si=O Double Bond and Formation of a Unique Pair of Sila-Hemiaminal and Silanoic Amide Tautomers. *J. Am. Chem. Soc.* **2010**, *132*, 6912−6913.

(6) (a) Li, L.; Fukawa, T.; Matsuo, T.; Hashizume, D.; Fueno, H.; Tanaka, K.; Tamao, K. A stable germanone as the first isolated heavy ketone with a terminal oxygen atom. *Nat. Chem.* **2012**, *4*, 361−365. (b) Sinhababu, S.; Yadav, D.; Karwasara, S.; Sharma, M. K.; Mukherjee, G.; Rajaraman, G.; Nagendran, S. The Preparation of Complexes of Germanone from a Germanium μ-Oxo Dimer. *Angew. Chem., Int. Ed.* **2016**, *55*, 7742−7746. (c) Sharma, M. K.; Sinhababu, S.; Mahawar, P.; Mukherjee, G.; Pandey, B.; Rajaraman, G.; Nagendran, S. Donor-acceptor-stabilised germanium analogues of acid chloride, ester, and acyl pyrrole compounds: synthesis and reactivity. *Chem. Sci.* **2019**, *10*, 4402−4411. (d) Sarkar, D.; Weetman, C.; Dutta, S.; Schubert, E.; Jandl, C.; Koley, D.; Inoue, S. N-Heterocyclic Carbene-Stabilized Germacylium Ion: Reactivity and Utility in Catalytic CO_2 Functionalizations. *J. Am. Chem. Soc.* **2020**, *142*, 15403−15411 Previously reported examples of Lewis base stabilized germanones:. (e) Yao, S.; Xiong, Y.; Driess, M. From NHC→germylenes to stable NHC→germanone complexes. *Chem. Commun.* **2009**, 6466−6468. (f) Yao, S.; Xiong, Y.; Wang, W.; Driess, M. Synthesis, Structure, and Reactivity of a Pyridine-Stabilized Germanone. *Chem.—Eur. J.* **2011**, *17*, 4890−4895.

(7) Filippou, A. C.; Baars, B.; Chernov, O.; Lebedev, Y. N.; Schnakenburg, G. Silicon-Oxygen Double Bonds: A Stable Silanone with a Trigonal-Planar Coordinated Silicon Center. *Angew. Chem., Int. Ed.* **2014**, *53*, 565−570.

(8) (a) Alvarado-Beltran, I.; Rosas-Sánchez, A.; Baceiredo, A.; Saffon-Merceron, N.; Branchadell, V.; Kato, T. A Fairly Stable Crystalline Silanone. *Angew. Chem., Int. Ed.* **2017**, *56*, 10481−10485. (b) Rosas-Sánchez, A.; Alvarado-Beltran, I.; Baceiredo, A.; Saffon-Merceron, N.; Massou, S.; Hashizume, D.; Branchadell, V.; Kato, T. Cyclic

(Amino)(Phosphonium Bora-Ylide)Silanone: A Remarkable Room-Temperature-Persistent Silanone. *Angew. Chem., Int. Ed.* **2017**, *56*, 15916−15920.
(9) (a) Wendel, D.; Reiter, D.; Porzelt, A.; Altmann, P. J.; Inoue, S.; Rieger, B. Silicon and Oxygen's Bond of Affection: An Acyclic Three-Coordinate Silanone and Its Transformation to an Iminosiloxysilylene. *J. Am. Chem. Soc.* **2017**, *139*, 17193−17198. (b) Reiter, D.; Frisch, P.; Szilvási, T.; Inoue, S. Heavier Carbonyl Olefination: The Sila-Wittig Reaction. *J. Am. Chem. Soc.* **2019**, *141*, 16991−16996.
(10) Kobayashi, R.; Ishida, S.; Iwamoto, T. An Isolable Silicon Analogue of a Ketone that Contains an Unperturbed Si = O Double Bond. *Angew. Chem., Int. Ed.* **2019**, *58*, 9425−9428.
(11) Selected review articles: (a) Xiong, Y.; Yao, S.; Driess, M. Chemical Tricks To Stabilize Silanones and Their Heavier Homologues with E═O Bonds (E=Si−Pb): From Elusive Species to Isolable Building Blocks. *Angew. Chem., Int. Ed.* **2013**, *52*, 4302−4311. (b) Loh, Y. K.; Aldridge, S. Acid-Base Free Main Group Carbonyl Analogues. *Angew. Chem., Int. Ed.* **2021**, *60*, 8626−8648. (c) Sun, T.; Li, J.; Wang, H. Recent Advances in the Chemistry of Heavier Group 14 Analogues of Carbonyls. *Chem.—Asian J.* **2022**, *17*, No. e202200611.
(12) (a) Zabula, A. V.; Pape, T.; Hepp, A.; Schappacher, F. M.; Rodewald, U. C.; Pöttgen, R.; Hahn, F. E. Trapping of Tin(II) and Lead(II) Homologues of Carbon Monoxide by a Benzannulated Lutidine-Bridged Bisstannylene. *J. Am. Chem. Soc.* **2008**, *130*, 5648−5649. (b) Gao, Y.; Yang, Y.; Zheng, W.; Su, Y.; Zhang, X.; Roesky, H. W. Germanium and Tin Monoxides Trapped by Oxophilic Germylene and Stannylene Ligands. *Inorg. Chem.* **2017**, *56*, 10220−10225.
(13) (a) Fischer, M.; Roy, M. M. D.; Wales, L. L.; Ellwanger, M. A.; Heilmann, A.; Aldridge, S. Structural Snapshots in Reversible Phosphinidene Transfer: Synthetic, Structural, and Reaction Chemistry of a Sn=P Double Bond. *J. Am. Chem. Soc.* **2022**, *144*, 8908−8913. (b) Fischer, M.; Roy, M. M. D.; Wales, L. L.; Ellwanger, M. A.; McManus, C.; Roper, A. F.; Heilmann, A.; Aldridge, S. Taming Heavier Group 14 Imine Analogues: Accessing Tin Nitrogen [Sn = N] Double Bonds and their Cycloaddition/Metathesis Chemistry. *Angew. Chem., Int. Ed.* **2022**, *61*, No. e202211616.
(14) See for example: (a) Chlupaty, T.; Padelkova, Z.; De Proft, F.; Willem, R.; Ruzicka, A. Addition of Lappert's Stannylenes to Carbodiimides, Providing a New Class of Tin(II) Guanidinates. *Organometallics* **2012**, *31*, 2203−2211. (b) Tacke, R.; Ribbeck, T. Bis(amidinato)- and bis(guanidinato)silylenes and silylenes with one sterically demanding amidinato or guanidinato ligand: synthesis and reactivity. *Dalton Trans.* **2017**, *46*, 13628−13659. (c) Ahmet, I. Y.; Thompson, J. R.; Johnson, A. L. Oxidative Addition to Sn^{II} Guanidinate Complexes: Precursors to Tin(II) Chalcogenide Nanocrystals. *Eur. J. Inorg. Chem.* **2018**, *2018*, 1670−1678.
(15) See the Supporting Information.
(16) (a) Pyykkö, P.; Atsumi, M. Molecular Single-Bond Covalent Radii for Elements 1−118. *Chem.—Eur. J.* **2009**, *15*, 186−197. (b) Pyykkö, P.; Atsumi, M. Molecular Double-Bond Covalent Radii for Elements Li-E112. *Chem.—Eur. J.* **2009**, *15*, 12770−12779.
(17) Chlupaty, T.; Ruzickova, Z.; Horacek, M.; Merna, J.; Alonso, M.; De Proft, F.; Ruzicka, A. Reactivity of Tin(II) Guanidinate with 1,2- and 1,3-Diones: Oxidative Cycloaddition or Ligand Substitution? *Organometallics* **2015**, *34*, 2202−2211.
(18) Yang, L.; Powell, D. R.; Houser, R. P. Structural variation in copper(I) complexes with pyridylmethylamide ligands: structural analysis with a new four-coordinate geometry index, τ_4. *Dalton Trans.* **2007**, 955−964.
(19) (a) Kuchta, M. C.; Parkin, G. Terminal Sulfido and Selenido Complexes of Tin: Syntheses and Structures of $[\eta^4$-$Me_8taa]SnE$ (E = S, Se). *J. Am. Chem. Soc.* **1994**, *116*, 8372−8373. (b) Leung, W.-P.; Kwok, W.-H.; Law, L. T. C.; Zhou, Z.-Y.; Mak, T. C. W. Synthesis and characterization of stannanechalcogenones; X-ray structures of $[R^N(R^N)Sn(\mu$-$S)]_2$ and $[(R^N)_2Sn = E]$ [R^N = $CH(SiMe_3)C_9H_6N$-8; E = Se, Te]. *J. Chem. Soc., Chem. Commun.* **1996**, 505−506. (c) Leung, W.-P.; Kwok, W.-H.; Zhou, Z.-Y.; Mak, T. C. W. Synthesis and Characterization of Group 14 Dialkylmetal Chalcogenones $R^N{}_2M = E$ [R^N = $CH(SiMe_3)C_9H_6N$-8 or $CPh(SiMe_3)C_5H_4N$-2; M = Ge or Sn; E = S, Se, or Te]. *Organometallics* **2000**, *19*, 296−303. (d) Saito, M.; Tokitoh, N.; Okazaki, R. Tin-Chalcogen Double-Bond Compounds, Stannanethione and Stannaneselone: Synthesis, Structure, and Reactivities. *J. Am. Chem. Soc.* **2004**, *126*, 15572−15582. (e) Chivers, T.; Eisler, D. J. Complete Chalcogenation of Tin(II) Centers in an Imidotin Cluster. *Angew. Chem., Int. Ed.* **2004**, *43*, 6686−6689. (f) Kirchmann, M.; Gädt, T.; Schappacher, F. M.; Pöttgen, R.; Weigend, F.; Wesemann, L. Partial double bond character in chalcogen compounds of stanna-closo-dodecaborate. *Dalton Trans.* **2009**, 1055−1062. (g) Mairychová, B.; Dostál, L.; Ruzicka, A.; Fulem, M.; Ruzicka, K.; Lycka, A.; Jambor, R. Intramolecularly Coordinated Stannanechalcogenones: X-ray Structure of $[2,6$-$(Me_2NCH_2)_2C_6H_3](Ph)Sn$ = Te. *Organometallics* **2011**, *30*, 5904−5910. (h) Bouska, M.; Strizik, L.; Dostal, L.; Ruzicka, A.; Lycka, A.; Benes, L.; Vlcek, M.; Prikryl, J.; Knotek, P.; Wagner, T.; Jambor, R. Mixed Organotin(IV) Chalcogenides: From Molecules to Sn-S-Se Semiconducting Thin Films Deposited by Spin-Coating. *Chem.—Eur. J.* **2013**, *19*, 1877−1881. (i) Park, J. H.; Kang, S. G.; Lee, Y. K.; Chung, T.-M.; Park, B. K.; Kim, C. G. Tin(II) Aminothiolate and Tin(IV) Aminothiolate Selenide Compounds as Single-Source Precursors for Tin Chalcogenide Materials. *Inorg. Chem.* **2020**, *59*, 3513−3517. (j) Sharma, M. K.; Glodde, T.; Neumann, B.; Stammler, H.-G.; Ghadwal, R. S. Distannabarrelenes with Three Coordinated Sn^{II} Atoms. *Chem.—Eur. J.* **2020**, *26*, 11113−11118. (k) Ruppert, H.; Greb, L. Calix[4]pyrrolato Stannate(II): A Tetraamido Tin(II) Dianion and Strong Metal-Centered σ-Donor. *Angew. Chem., Int. Ed.* **2022**, *61*, No. e202116615. (l) Hossain, J.; Parvin, N.; Shah, B. K.; Khan, S. Four-Coordinate Germylene and Stannylene and their Reactivity towards Se & Te. *Z. Anorg. Allg. Chem.* **2022**, *648*, No. e202200164.
(20) It is worth noting that tin cubane complexes with four-coordinate tin centres and terminal selenium bonds are reported in literature: (a) Chivers, T.; Clark, T. J.; Krahn, M.; Parvez, M.; Schatte, G. Cubane Complexes with Two (or More) Group 14-Group 16 Double Bonds: Syntheses and X-ray Structures of $Sn_4Se_2(NtBu)_4$ and $Ge_4Se_3(NtBu)_4$. *Eur. J. Inorg. Chem.* **2003**, *2003*, 1857−1860. (b) Chivers, T.; Eisler, D. J.; Ritch, J. S. Chalcogenide Derivatives of the seco-Cubane $[Sn_3(\mu_2$-$NHtBu)_2(\mu_2$-$NtBu)(\mu_3$-$NtBu)]$. *Z. Anorg. Allg. Chem.* **2004**, *630*, 1941−1946. (c) Eisler, D. J.; Chivers, T. Chalcogenide Derivatives of Imidotin Cage Complexes. *Chem.—Eur. J.* **2006**, *12*, 233−243.
(21) ^{77}Se satellites in the $^{119}Sn\{^1H\}$ NMR and $^{117/119}Sn$ satellites in the ^{77}Se NMR were not observed.
(22) Ishida, S.; Abe, T.; Hirakawa, F.; Kosai, T.; Sato, K.; Kira, M.; Iwamoto, T. Persistent Dialkylsilanone Generated by Dehydrobromination of Dialkylbromosilanol. *Chem.—Eur. J.* **2015**, *21*, 15100−15103.
(23) (a) Schulz, A.; Thomas, M.; Villinger, A. Tetrazastannoles versus distannadiazanes - a question of the tin(II) source. *Dalton Trans.* **2019**, *48*, 125−132. (b) Simons, R. S.; Pu, L.; Olmstead, M. M.; Power, P. P. Synthesis and Characterization of the Monomeric Diaryls $M\{C_6H_3$-2,6-$Mes_2\}_2$ (M = Ge, Sn, or Pb; Mes = 2,4,6-$Me_3C_6H_2$-) and Dimeric Aryl-Metal Chlorides $[M(Cl)\{C_6H_3$-2,6-$Mes_2\}]_2$ (M = Ge or Sn). *Organometallics* **1997**, *16*, 1920−1925.
(24) (a) Tokitoh, N.; Matsuhashi, Y.; Okazaki, R. Novel synthesis and molecular structure of tetraselenastannolanes. *Tetrahedron Lett.* **1991**, *32*, 6151−6154. (b) Matsuhashi, Y.; Tokitoh, N.; Okazaki, R.; Goto, M.; Nagase, S. Synthesis and Structure of 1,2,3,4,5-Tetrachalcogenastannolanes. *Organometallics* **1993**, *12*, 1351−1358.
(25) Addison, A. W.; Rao, T. N.; Reedijk, J.; van Rijn, J.; Verschoor, G. C. Synthesis, structure and spectroscopic properties of copper(II) compounds containing nitrogen-sulphur donor ligands; the crystal and molecular structure of aqua[1,7-bis(N-metyhlbenzimidazol-2'-yl)-2,6-dithiaheptane]copper(II) perchlorate. *J. Chem. Soc., Dalton Trans.* **1984**, 1349−1356.
(26) Spek, A. L. PLATOn SQUEEZE: a tool for the calculation of the disordered solvent contribution to the calculated structure factors. *Acta Crystallogr.* **2015**, *71*, 9−18.
(27) Bruker AXS Inc. *Bruker Apex CCD, SAINT*, v8.40B; Bruker AXS Inst. Inc.: WI, USA, Madison, 2019.
(28) Krause, L.; Herbst-Irmer, R.; Sheldrick, G. M.; Stalke, D. Comparison of silver and molybdenum microfocus X-ray sources for

https://doi.org/10.1021/acs.inorgchem.4c00598
Inorg. Chem. 2024, 63, 7455−7463

single-crystal structure determination. *J. Appl. Crystallogr.* **2015**, *48*, 3−10.
(29) Sheldrick, G. M. SHELXT - Integrated space-group and crystal-structure determination. *Acta Crystallogr.* **2015**, *71*, 3−8.
(30) Sheldrick, G. M. Crystal structure refinement with SHELXL. *Acta Crystallogr.* **2015**, *71*, 3−8.
(31) Dolomanov, O. V.; Bourhis, L. J.; Gildea, R. J.; Howard, J. A.; Puschmann, H. OLEX2: a complete structure solution, refinement and analysis program. *J. Appl. Crystallogr.* **2009**, *42*, 339−341.
(32) Hübschle, C. B.; Sheldrick, G. M.; Dittrich, B. ShelXle: a Qt graphical user interface for SHELXL. *J. Appl. Crystallogr.* **2011**, *44*, 1281−1284.
(33) Parsons, S.; Flack, H.; Wagner, T. Use of intensity quotients and differences in absolute structure refinement. *Acta Crystallogr.* **2013**, *69*, 249−259.
(34) Groom, C. R.; Bruno, I. J.; Lightfoot, M. P.; Ward, S. C. The Cambridge Structural Database. *Acta Crystallogr.* **2016**, *72*, 171−179.
(35) Frisch, M. J.; Trucks, G. W.; Schlegel, H. B.; Scuseria, G. E.; Robb, M. A.; Cheeseman, J. R.; Scalmani, G.; Barone, V.; Petersson, G. A.; Nakatsuji, H.; Li, X.; Caricato, M.; Marenich, A. V.; Bloino, J.; Janesko, B. G.; Gomperts, R.; Mennucci, B.; Hratchian, H. P.; Ortiz, J. V.; Izmaylov, A. F.; Sonnenberg, J. L.; Williams-Young, D.; Ding, F.; Lipparini, F.; Egidi, F.; Goings, J.; Peng, B.; Petrone, A.; Henderson, T.; Ranasinghe, D.; Zakrzewski, V. G.; Gao, J.; Rega, N.; Zheng, G.; Liang, W.; Hada, M.; Ehara, M.; Toyota, K.; Fukuda, R.; Hasegawa, J.; Ishida, M.; Nakajima, T.; Honda, Y.; Kitao, O.; Nakai, H.; Vreven, T.; Throssell, K.; Montgomery, J. A., Jr; Peralta, J. E.; Ogliaro, F.; Bearpark, M. J.; Heyd, J. J.; Brothers, E. N.; Kudin, K. N.; Staroverov, V. N.; Keith, T. A.; Kobayashi, R.; Normand, J.; Raghavachari, K.; Rendell, A. P.; Burant, J. C.; Iyengar, S. S.; Tomasi, J.; Cossi, M.; Millam, J. M.; Klene, M.; Adamo, C.; Cammi, R.; Ochterski, J. W.; Martin, R. L.; Morokuma, K.; Farkas, O.; Foresman, J. B.; Fox, D. J. *Gaussian 16*, Revision A.03; Gaussian, Inc.: Wallingford, CT, 2016.
(36) Becke, A. D. Density-functional exchange-energy approximation with correct asymptotic behavior. *Phys. Rev. A* **1988**, *38*, 3098−3100.
(37) Perdew, J. P. Density-functional approximation for the correlation energy of the inhomogeneous electron gas. *Phys. Rev. B: Condens. Matter Mater. Phys.* **1986**, *33*, 8822−8824.
(38) Weigend, F.; Ahlrichs, R. Balanced basis sets of split valence, triple zeta valence and quadruple zeta valence quality for H to Rn: Design and assessment of accuracy. *Phys. Chem. Chem. Phys.* **2005**, *7*, 3297−3305.
(39) Grimme, S.; Antony, J.; Ehrlich, S.; Krieg, H. A consistent and accurate ab initio parametrization of density functional dispersion correction (DFT-D) for the 94 elements H-Pu. *J. Chem. Phys.* **2010**, *132*, 154104.
(40) Grimme, S.; Ehrlich, S.; Goerigk, L. Effect of the damping function in dispersion corrected density functional theory. *J. Comput. Chem.* **2011**, *32*, 1456−1465.
(41) Glendening, E. D.; Badenhoop, J. K.; Reed, A. E.; Carpenter, J. E.; Bohmann, J. A.; Morales, C. M.; Karafiloglou, P.; Landis, C. R.; Weinhold, F. *Theoretical Chemistry Institute NBO 7.0*; University of Wisconsin: Madison, WI, 2018.

https://doi.org/10.1021/acs.inorgchem.4c00598
Inorg. Chem. 2024, 63, 7455−7463